Physics of Plasmas ARTICLE scitation.org/journal/php

# Numerical study of coronal plasma jet formation

Cite as: Phys. Plasmas **28**, 012901 (2021); doi: 10.1063/5.0025136
Submitted: 15 August 2020 · Accepted: 7 December 2020 ·
Published Online: 6 January 2021



J. Latham,[1,a)] E. V. Belova,[2] and M. Yamada[2]

## AFFILIATIONS

[1]Department of Physics, Princeton University, Princeton, New Jersey 08544, USA
[2]Princeton Plasma Physics Laboratory, Princeton, New Jersey 08543, USA

[a)]**Author to whom correspondence should be addressed:** joshla@umich.edu. **Present address:** Department of Nuclear Engineering and Radiological Sciences, University of Michigan, Ann Arbor, Michigan 48109, USA.

## ABSTRACT

A new scenario for solar flare eruption in the coronal holes is analyzed by using MHD stability concepts for a spheromak configuration. The stability properties of a spheromak partially embedded into a conducting surface are studied using three dimensional MHD simulations. In agreement with the analytical theory, a large degree of line-tying stabilizes the spheromak's tilt instability, while the elongation has a destabilizing effect. High-resolution nonlinear simulations also demonstrate current sheet formation at the upper surface of the spheromak, where the tilted magnetic field of the spheromak reconnects with the background magnetic field. The calculated stability threshold and the observed magnetic reconnection support a model of coronal jet eruptions where a dome-like magnetic structure grows through flux emergence on the solar surface, tilts, reconnects, and erupts. Countering the effect from elongation, line-tying strongly stabilizes a spheromak growing from a flux-emergence process, suggesting that to accelerate the onset of eruptive coronal jets, there must be magnetic reconnection at the bottom of the spheromak to detach the structure from the solar surface.





## I. INTRODUCTION

Space-based solar observations revealed that the solar atmosphere is full of small scale flares, called micro-flares, and the associated coronal jets, particularly prominent in the coronal holes. One such example is the coronal x-ray jets discovered by Yohkoh/SXT.[1] The type of x-ray jets, called anemone jets, are preceded by dome-shaped magnetic structures, visible at the jet footpoint in soft x-ray images of the eruption process.[2,3] Shibata dubbed these dome-shaped structures "anemones" because of the fan shape of the magnetic field, similar to that of a sea anemone. There are many pieces of observational evidence that show that the anemone jets are produced by magnetic reconnection.[2] Yokoyama and Shibata[1,4] performed the first 2D MHD simulation of reconnection between an emerging flux and an overlying coronal field, explaining many of the observational characteristics.

Since then, numerous simulation studies have led to a general consensus that the eruptions leading to the generation of x-ray jets result from magnetic reconnection in the solar corona.[5–9] Two possible scenarios leading to the reconnection have been investigated in detail. One is based on a 2D flux emergence scenario of Yokoyama and Shibata.[4] However, it is not clear how this scenario would lead to an approximately axially symmetric structure in a full 3D geometry. The second is related to an onset of kink type instability in twisted magnetic field lines formed due to prescribed circular footpoint motion of a given initial magnetic configuration.[10,11] Therefore, while the eruptive/reconnection stage of jet formation was studied in sufficient detail and agrees well with observations,[6] much less attention was paid to the formation of the initial magnetic configuration. The exact mechanism of its formation remains unknown. A new model of the "anemone" as a spheromak partially embedded onto the solar surface was proposed by Yamada.[12] The goal of this work is to investigate the feasibility of this concept, as well as possible roles of the related ideal MHD instabilities and reconnection as applied to coronal x-ray jet generation.

A spheromak is one of the well explored fusion configurations,[13] which, in the low plasma pressure limit, is basically a simply connected force-free magnetic vortex. In a closed system, the turbulent plasma will relax into a spheromak configuration with $\nabla \times \mathbf{B} = \lambda \mathbf{J}$ (Taylor state[14]), minimizing the system energy while conserving a total helicity. Experimentally, the spheromak can be formed by a helicity injection,[15,16] for example, by a magnetized coaxial gun. The formation mechanism relies on 3D dynamo action for converting injected toroidal flux into poloidal flux. The 3D instabilities and reconnection subsequently lead to a closed field line configuration.[16,17]

In the external field, the spheromak can be unstable to the tilt instability,[18–20] as it tends to flip to align its magnetic moment with

the background magnetic field. In laboratory experiments, the tilting can be stabilized by shaping or conducting surfaces providing stabilizing surface currents near the spheromak.[18–20] Another source of stabilization comes from the line-tying of the magnetic field.[21,22]

A spheromak partially embedded onto the solar surface has the magnetic topology similar to that of the solar "anemone." Therefore, in this paper, we explore the line-tying stabilization of the spheromak's tilt mode in a new geometry, relevant to coronal jets. 3D MHD simulations are used to investigate the stability properties of spheromaks where the magnetic field lines on the one side are tied to a conducting surface. This is relevant for solar applications because the "anemone" dome-structures, if they are to be modeled as spheromaks, are embedded to the solar surface and are thus line-tied within the separatrix.

This paper is organized as follows: Section II describes the simulation model. Section III describes results of 3D linearized MHD simulations of the tilt instability of the spheromak line-tied to a surface, while Sec. IV describes results of nonlinear simulations demonstrating nonlinear evolution of the tilt mode. Discussion and conclusions are given in Sec. V.

## II. SIMULATION MODEL

The HYbrid/MHD code (HYM)[23] has been used to investigate the linear stability properties and nonlinear evolution of a line-tied spheromak. The HYM code is an initial value, 3D nonlinear, global stability code using an arbitrary orthogonal coordinate system and different physics models. The code version used in this work utilizes the one-fluid resistive MHD model in the cylindrical geometry.

In the HYM code, a second-order, time centered, explicit scheme is used for time stepping. Fourth-order finite difference and cylindrical geometry are used to advance fields and apply boundary conditions. For a typical linearized run, a cylindrical $(Z, R, \phi)$ grid is used, and a finer grid is used in the nonlinear simulations. For simplicity, the uniform background plasma density is assumed. Perfectly conducting boundary conditions are applied to the perturbed fields at the simulation boundaries.

Initial conditions have been generated using the Grad–Shafranov solver for a very small value of beta $\beta = 0.002 - 0.02$ (ratio of plasma to magnetic pressure), resulting in a nearly force-free initial configuration. The tilt instability is studied for spheromaks of various elongations, where the elongation is defined as the ratio of the separatrix length to its radius ($L$ and $R$, respectively) (Fig. 1). The effect of line-tying to a conducting surface is modeled by placing one of the axial boundaries very close to the spheromak. In most of the cases considered here, the conducting surface is crossing the separatrix, so that part of the spheromak internal flux is line-tied to a wall (Fig. 1). In this paper, the line-tying effect is quantified by $\chi \equiv \psi_{tied}/\psi_0$, where $\psi_{tied}$ is the poloidal magnetic flux between the separatrix and the largest closed flux surface and $\psi_0$ is the flux passing between the separatrix and the magnetic axis (Fig. 1). Thus, $\chi$ is the ratio of the tied flux of the spheromak to the total flux of the spheromak. The degree of line-tying is varied by moving the bottom conducting boundary closer to the spheromak center.

The linear simulations were run for Lundquist number $S \sim 10^5$, which is much smaller than the realistic values for the corona. However, the tilt instability is an ideal MHD mode, which is very weakly affected by finite resistivity (for the used values of $S \gg 1$).

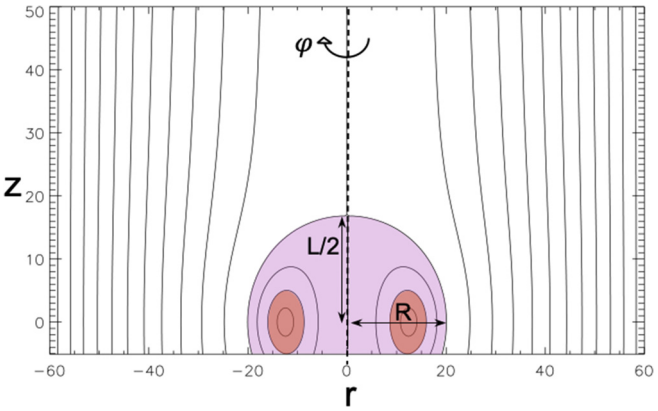


**FIG. 1.** Contour plot of the poloidal flux for a spheromak in the external magnetic field, showing a $z$–$r$ cross section. The spheromaks of the simulation varied in elongation $\varepsilon \equiv L/R$. The figure shows asymmetric line-tying of spheromak. The violet area represents the flux of the spheromak which is *tied* to the conducting boundary ($\psi_{tied}$), and the red represents the flux which is *untied*, which together adds to the total flux of the spheromak ($\psi_{tied} + \psi_{untied} = \psi_0$).

For nonlinear simulations including the magnetic reconnection, two models were used. One with uniform resistivity corresponding to $S \sim 2 \times 10^4$ and an anomalous resistivity model similar to that used by Yokoyama and Shibata[4] (also Sato and Hayashi[24]). In both cases, the reconnection time scales were similar and determined by the tilt evolution timescale.

The HYM code has been verified against an analytic threshold for the $n = 1$ tilt stability and the numerically calculated growth rates of Finn and Bondeson for a wall-confined cylindrical spheromak solution with no background magnetic field.[19,20] For this paper, however, in order to model the "anemone" dome on the solar surface, spheromaks set in a background magnetic field with asymmetric line-tying are considered. The simulation box sizes (both radius and length) were increased until the converged results have been obtained, corresponding to spheromak stability in a half-plane.

## III. LINEAR RESULTS

In a cylindrical flux conserver, without the applied external field, the spheromak is stable to the $n = 1$ tilt mode when its elongation is sufficiently small ($\varepsilon = L/R < 1.67$),[19,20] and where $n$ is the toroidal Fourier harmonic number. External field has a destabilizing effect, reducing the stability threshold to $\varepsilon \lesssim 1.4$. It has been previously shown that line-tying effects can stabilize the tilt mode in a spheromak with larger elongation and surrounded by the external field.[21] These calculations found that the line-tying of the external field lines allowed the axial (z-direction) conducting boundaries and radial conducting boundary to be placed further away from the spheromak while still maintaining stability. However, these studies were focused on laboratory (fusion) applications and differed from astrophysically relevant plasmas in two important ways. First, the up–down symmetry of the conducting box was assumed. Second, the conducting boundaries were placed outside of the separatrix to avoid the confined plasma touching the vessel wall.

Asymmetric line-tying has been studied in simulations of laboratory spheromak formation, in which case the spheromak was line-tied

to the plasma gun.[22] In these simulations, the spheromak shape and stability properties were determined by the shape of the flux conserver, which had a small aspect ratio $L_c/R_c \leq 1.6$ (corresponding to a tilt stable regime) and did not include the external field. Previous laboratory experiments of line-tied spheromaks[25] studied the spheromak formation and expansion into a large vacuum chamber. Since the ambient field was not applied, these spheromaks were tilt stable, in contrast to the present study.

For a solar case, the spheromak configuration of interest does not have up–down symmetry—there is only one line-tying boundary, the solar surface. In addition, this boundary cuts through the separatrix, creating a dome-like structure in the corona, while tying-up a part of the spheromak's internal flux. In the simulations, this was modeled by placing the bottom of the simulation box very close to the spheromak, crossing the separatrix, and moving all other boundaries further away until the converged results were obtained. Two parameters were changed in a set of linearized 3D MHD simulations: (1) the elongation of the spheromak and (2) the amount of poloidal flux within the spheromak separatrix that was line-tied to the solar surface.

Figure 2 shows the calculated linear growth rate of the $n = 1$ tilt mode against the line-tying fraction $\chi$ (defined as $\psi_{tied}/\psi_0$, where $\psi_{tied}$ is the poloidal magnetic flux of the spheromak, which pierces the conducting boundary, and $\psi_0$ is the total poloidal flux of the spheromak, as in Fig. 1). The growth rate $\gamma$ is normalized by the Alfvén time $\tau_A \equiv R/v_A$, where $R$ is the separatrix radius and $v_A$ is the Alfvén speed. For each elongation of the spheromak ($\varepsilon = 1.43, 1.69, 1.96, 2.75$), the growth rate of the $n = 1$ mode was calculated for an ensemble of line-tying fractions ranging from $\chi = 0$ to $\chi = 1$, where a case of $\chi = 1$ corresponds to a boundary crossing the spheromak in the middle (through the magnetic axis).

For each elongation, there was a particular amount of tied flux at which the spheromak transitioned from unstable to stable; this stability threshold, $\chi_*$, in Fig. 3, is, in Fig. 2, the point where the growth rate curve hits $\gamma\tau_A = 0$. The stability threshold $\chi_*$ increases with the elongation of the spheromak, ranging from 0.14 ($\varepsilon = 1.4$) to $\chi_* = 0.78$ (for the largest elongation considered $\varepsilon = 2.75$). Thus, the linearized

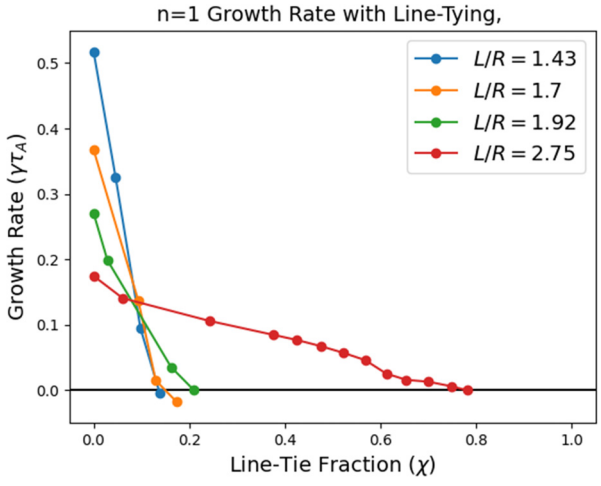


**FIG. 2.** Curves of the growth rate of the n = 1 tilt mode vs the line-tying fraction $\chi \equiv \psi_{tied}/\psi_0$, for different elongations of spheromak $\varepsilon \equiv L/R$.

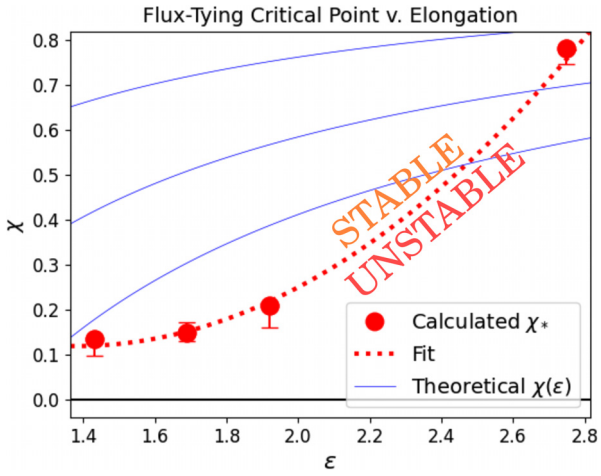


**FIG. 3.** The critical line-tying fraction $\chi_*$ vs the elongation of the spheromak. Error bars are the margin between zero-crossing-point and the adjacent data point's $\chi$ value in Fig. 2. Curves of $\chi(\varepsilon)$ (blue) show approximate relation between elongation and line-tying for a flux-emergence scenario.

simulations demonstrate that the spheromak configuration partially embedded into the solar surface can remain stable with respect to the tilt as long as its elongation remains relatively small, and the line-tying is sufficiently strong, and it will be destabilized if either its elongation is increased or the fraction of the line-tied flux is reduced below the threshold.

Since a magnetic configuration on the surface of the sun is not enclosed in a conducting box, the size of the simulation region was increased to ensure that the results of our simulations converge. The results of this test are summarized in Table I where the relative simulation box size is represented by $R_c/R$ ($R_c$ is the radius of the simulation boundary and $R$ is the radius of the separatrix). The ratio of simulation z axis length to separatrix length $L$ roughly followed $R_c/R$. The

**TABLE I.** Convergence of threshold for expanding boundary. $\varepsilon = L/R$ spheromak elongation; $R_c$ = radius of conducting boundary; $R$ = radius of spheromak; $z_c$ = distance from the center of spheromak to upper axial boundary; $L$ = axial length of spheromak; and $\chi_*$ = critical line-tying fraction for stability.

| $\varepsilon$ | $R_c/R$ | $2z_c/L$ | $\chi_*$ |
|---|---|---|---|
| 1.43 | 1.18 | 1.37 | 0.0 |
| 1.43 | 1.50 | 2.09 | 0.13 |
| 1.43 | 2.23 | 3.11 | 0.14 |
| 1.69 | 1.18 | 1.12 | 0.18 |
| 1.68 | 1.49 | 1.77 | 0.15 |
| 1.69 | 2.23 | 2.65 | 0.15 |
| 1.96 | 1.21 | 1.78 | 0.25 |
| 1.96 | 1.61 | 1.65 | 0.23 |
| 1.92 | 2.40 | 2.50 | 0.21 |
| 2.75 | 1.06 | 1.13 | 0.52 |
| 2.75 | 1.73 | 1.26 | 0.74 |
| 2.75 | 2.59 | 1.88 | 0.78 |

simulations were performed for four different values of elongation, where the elongation was changed by changing the spheromak toroidal field profile taken in the form: $RB_\phi \sim \psi^\sigma$. For approximately the same value of the spheromak elongation, the critical line-tying fraction $\chi_*$ was found to converge as the box size increased. This convergence indicates that the simulation results are valid for sufficiently large simulation box, approaching a half-infinite domain.

## IV. NONLINEAR 3D SIMULATIONS

3D nonlinear simulations have been performed showing the evolution of the tilt instability in the case of an unstable spheromak. The high resolution simulations (grid size is $nz \times nr \times n\phi = 240 \times 190 \times 64$) include the nonlinear interaction of all the toroidal harmonics. Simulations were performed for spheromaks of the elongation $\varepsilon = 1.67$ and the line-tied fraction $\chi = 11\%$. (For this elongation, the stability threshold $\chi_*$ is 15%, so this case is linearly unstable.) The nonlinear simulation was allowed to run until the spheromak was tilted at a relatively large angle, when the spheromak plasma and current came into contact with the conducting surface.

The simulation results that show the earlier stages of tilting are shown in Figs. 4 and 5(b). Figure 4 shows the contour plot of the toroidal component of the plasma current, with blue/red color indicating the direction in/out of the page. The contour plot is drawn in the plane of the tilt. Black arrows represent flow velocity, with a maximum value of $v = 0.039 v_A$, where the Alfvén velocity is defined in terms of the magnetic field at the center of the spheromak and the background density. The tilting motion is clockwise. The tilting of the spheromak is also apparent in Fig. 5, where the 3D magnetic field lines of the spheromak are plotted for two time frames of the same non-linear simulation as Fig. 4. An internal flux surface is covered by the multicolor (mostly green) field line. In blue, curving around the spheromak and extending upwards are the field lines of the ambient magnetic field.

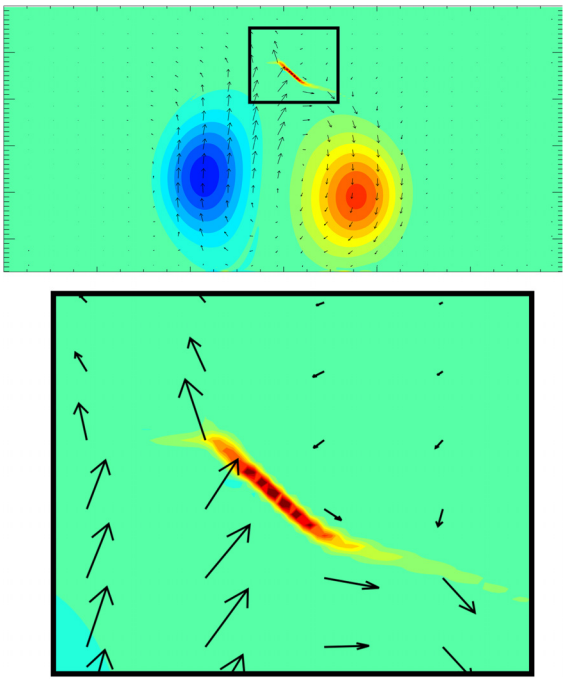

**FIG. 4.** Contour plot of plasma current, where the colors indicate the current direction in or out of the page. Black arrows represent flow velocity. Current sheet formation is visible at the top, close to the separatrix. Simulation parameters are $\varepsilon = 1.67$, $\chi = 11\%$. The close-up on the current sheet by the separatrix shows that the left half of the spheromak, which tilts upwards, flows into the current sheet and forces the reconnection between the spheromak's magnetic field and the background field. It should be noted that the current sheet appears at the left hand side (the opposite side of tilting) of the major axis of the inner spheromak.

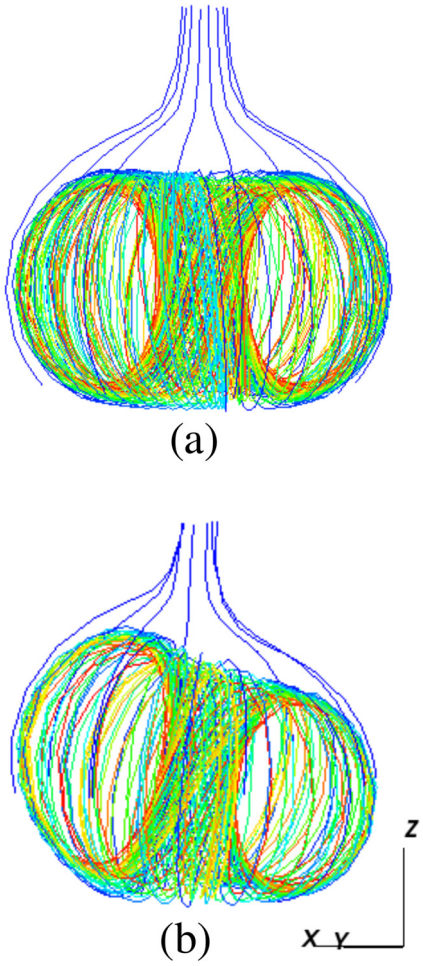


**FIG. 5.** Field lines of tilting spheromak. Field lines were chosen to help visualize the separatrix. An internal flux surface near the separatrix is covered by the multicolor (mostly green) field line. In blue, curving around the spheromak and extending upwards are the field lines of the ambient magnetic field. Figures drawn with VisIt program, from simulation data. (a) depicts the field lines at $t = 0$, while (b) depicts field lines at the same time as Fig. 4.

When the spheromak tilts, the magnetic field lines from the top of the tilted spheromak oppose the external field lines, resulting in an appearance of the reconnection layer. The current sheet formation is visible at the top of the spheromak close to the separatrix in Fig. 4. The close-up on the current sheet shows that the left half of the spheromak, which tilts upwards, flows into the current sheet. This tilting motion

forces the flux pileup, and a very steep gradient of the magnetic field develops across the current layer. The resulting nearly Alfvénic outflows from the current sheet are obtained in the later stages of the spheromak tilting, as shown in Fig. 6. Here, vector plots show flow velocity, and color contour plot shows the velocity magnitude normalized to Alfvén velocity. All plots are drawn approximately in the plane of the tilt. Similar to Fig. 4, the clockwise motion of the spheromak corresponds to the tilt motion, while larger magnitude flows localized near the x-points are the reconnection outflows. The peak values of the up-down outflow velocity are approximately $0.5v_A$ and $-0.9v_A$.

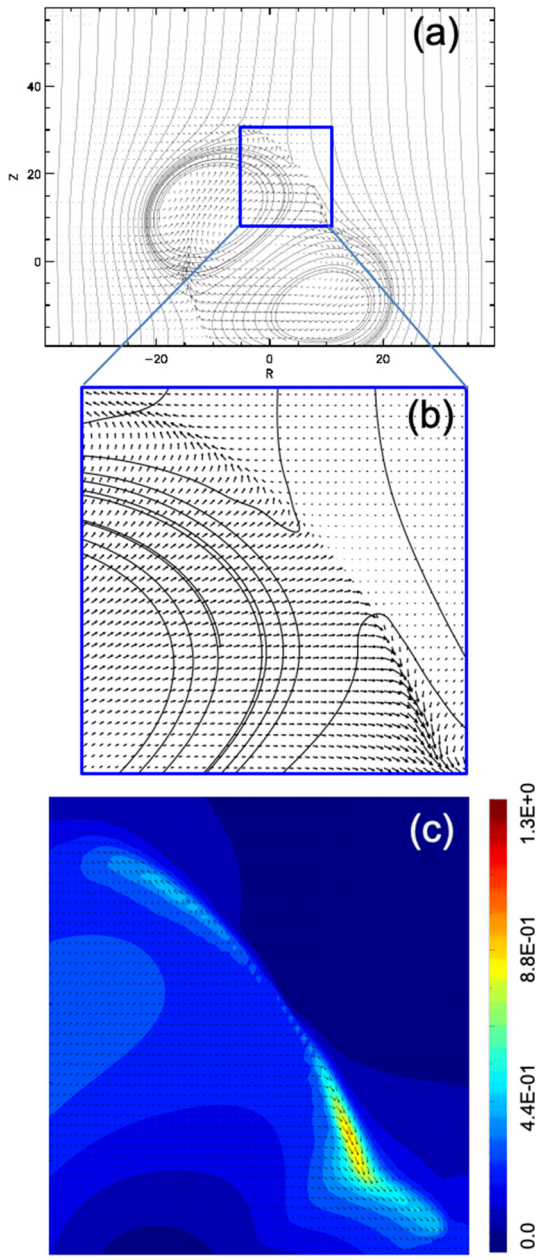


**FIG. 6.** Vector plots show flow velocity; black lines display magnetic field integrated only by ($B_R$, $B_Z$) components in the plane (not the full 3D magnetic field lines). (a) The top reconnection region is marked with the rectangular box, and x-point is located near the center of the box. (b) and (c) The zoomed-in plots show reconnection region in higher resolution. Color contour plot shows velocity magnitude normalized to Alfvén velocity.

As the spheromak magnetic field lines reconnect with the external field, the plasma gets accelerated by the straightening magnetic field lines (by the so-called "slingshot effect"[26]). If continued, the reconnection would rip apart the spheromak, releasing magnetic energy along the open field lines.

## V. DISCUSSION AND CONCLUSION

Numerical simulations performed in this work have demonstrated that spheromak formation, growth, and tilting instability can be a plausible explanation for the observed solar surface structures called "anemones." It was demonstrated, in particular, that a spheromak can exist stably if it is line-tied to a conducting surface, which means it could be an appropriate magnetic configuration for x-ray jets in the solar corona. For elongations from $\varepsilon = 1.4$ to $\varepsilon \sim 3$, the fraction of line-tied flux needed for stability ranges from $\chi_* = 0.14$ to $\chi_* = 0.78$, and the instability threshold increases with the elongation (Fig. 3).

A line-tied spheromak on the solar surface can elongate by the injection of poloidal and toroidal flux from the photosphere. The injected flux creates an increased magnetic pressure inside, which can push the spheromak upwards. The increased elongation would destabilize the spheromak, while at the same time the line-tying of the newly emerged flux would have a stabilizing effect on the $n = 1$ tilt mode.

Assuming that the length of the spheromak is linearly proportional to the poloidal flux, and also that the radius does not change significantly as flux is injected, the relation between $\chi$ and $\varepsilon$ as a spheromak grows through line-tied flux injection can be approximated as $\chi(\varepsilon) = 1 - \frac{a}{\varepsilon^2}$, where $a$ is a constant dependent on the initial values of $\chi$ and $\varepsilon$. This dependence is shown in Fig. 3 for different values of $a$, where the blue lines represent the trajectory through $\chi$–$\varepsilon$ space as the spheromak grows. Figure 3 shows that any spheromak will eventually cross the line-tying stability threshold by the elongation from flux-emergence alone. However, relatively large elongation $\varepsilon \gtrsim 2.5$ will be needed for instability.

One possibility for how a flux-injected spheromak can become unstable more quickly is if the injected flux becomes untied. This would require magnetic reconnection at the *bottom* of the spheromak, detaching it from the conducting surface (Fig. 7). (This process would be similar to 3D relaxation and reconnection during helicity injection in a laboratory spheromak.[16,17]) Reduction of $\chi$ through bottom reconnection could move the spheromak past the stability threshold quickly for any elongation.

The above considerations, therefore, suggest an important conclusion that in order for a semi-spheromak structure in the solar corona to become unstable for eruption, there must be magnetic reconnection between the photosphere and the spheromak to detach the emerging flux, which would otherwise stabilize the spheromak via line-tying effects.

In summary, MHD simulations were carried out to examine the dependence of the spheromak tilt instability on elongation and line-tying for application to x-ray bursts from a dome shaped solar flare in

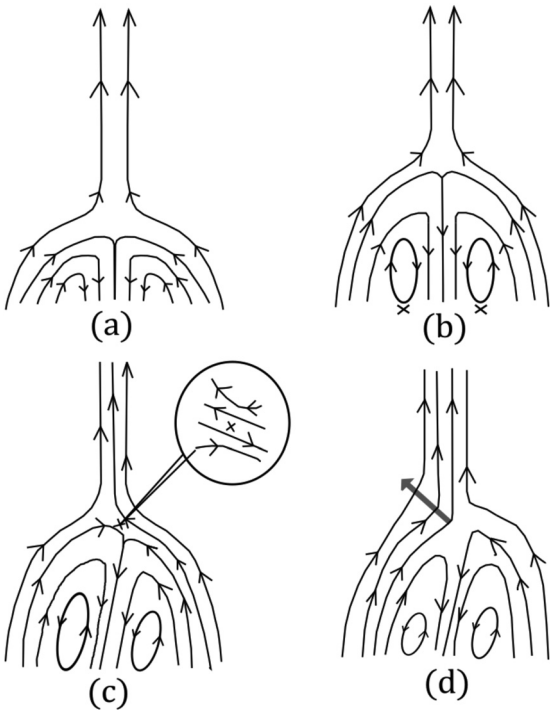


**FIG. 7.** Reconnection happens first at the bottom (b) detaching part of the flux from the surface and forming closed spheromak surfaces, leading to reduction of tied flux and tilting instability. After significant tilting, the reconnection starts at the top (c).

a coronal hole of the sun. It was found that a small amount of line-tying was sufficient to stabilize moderately oblate spheromaks, and significantly more line-tying was necessary to stabilize very elongated spheromaks. It was verified that these results hold for a single-plane line-tying boundary such as the photosphere. It was suggested that the line-tying effects could restrain an anemone spheromak from undergoing a tilt instability unless there is magnetic reconnection to detach emerging flux from the solar surface.

The formation of an anemone x-ray jet proceeds as follows: An anemone configuration on the sun grows from the flux-emergence out of the solar surface and 3D relaxation. Magnetic reconnection on the bottom of the spheromak reduces the fraction of the line-tied flux, a process that is sped up by the higher resistivity in the cooler and much denser plasma at the solar surface. When the flux-emergence and bottom-reconnection cause elongation and the reduction of line-tying past stability threshold, the tilting of the spheromak occurs, causing upper reconnection with the open field lines at the separatrix. This ejects the spheromak's energy and plasma into the open field lines, producing the well-known soft x-ray emission pattern.

## ACKNOWLEDGMENTS

The simulations reported here were carried out using resources of the National Energy Research Scientific Computing Center (NERSC). This research was supported by the U.S. Department of Energy Contract No. DE-AC02–09CH11466.

## DATA AVAILABILITY

The data that support the findings of this study are available from the corresponding author upon request.

## REFERENCES

[1]K. Shibata, S. Nozawa, and R. Matsumoto, "Magnetic reconnection associated with emerging magnetic flux," Publ. Astron. Soc. Jpn. **44**, 265 (1992), available at http://articles.adsabs.harvard.edu/full/1992PASJ...44..265S
[2]K. Shibata, T. Nakamura, T. Matsumoto, K. Otsuji, T. Ueno, R. Kitai, S. Nozawa, S. Tsuneta, Y. Suematsu, K. Ichimoto, T. Shimizu, Y. Katsukawa, T. D. Tarbell, T. E. Berger, B. W. Lites, R. A. Shine, and A. M. Title, "Chromospheric anemone jets as evidence of ubiquitous reconnection," Science **318**, 1591 (2007).
[3]B. Filippov, L. Golub, and S. Koutchmy, "X-ray jet dynamics in a polar coronal hole region," Sol. Phys. **254**, 259 (2009).
[4]T. Yokoyama and K. Shibata, "Numerical simulation of solar coronal x-ray jets based on the magnetic reconnection model," Publ. Astron. Soc. Jpn. **48**, 353 (1996).
[5]P. F. Wyper, S. K. Antiochos, and R. DeVore, "A universal model for solar eruptions," Nature **544**, 452–455 (2017).
[6]N. E. Raouafi, S. Patsourakos, E. Pariat, P. R. Young, A. C. Sterling, A. Savcheva, M. Shimojo, F. Moreno-Insertis, C. R. DeVore, V. Archontis, T. Török, H. Mason, W. Curdt, K. Meyer, K. Dalmasse, and Y. Matsui, "Solar coronal jets: Observations, theory, and modeling," Space Sci. Rev. **201**, 1 (2016).
[7]A. C. Sterling, R. L. Moore, D. A. Falconer, and M. Adams, "Small-scale filament eruptions as the driver of x-ray jets in solar coronal holes," Nature **523**, 437 (2015).
[8]P. Devi, B. Joshi, R. Chandra, P. K. Mitra, A. M. Veronig, and R. Joshi, "Development of a confined circular-cum-parallel ribbon flare and associated pre-flare activity," Sol. Phys. **295**, 75 (2020).
[9]S. S. Nayak, R. Bhattacharyya, A. Prasad, Q. Hu, S. Kumar, and B. Joshi, "A data-constrained magnetohydrodynamic simulation of successive events of blowout jet and c-class flare in NOAA AR 12615," Astrophys. J. **875**, 10 (2019).
[10]K. A. Meyer, A. S. Savcheva, D. H. Mackay, and E. E. DeLuca, "Nonlinear force-free modeling of solar coronal jets in theoretical configurations," Astrophys. J. **880**, 62 (2019).
[11]E. Pariat, S. K. Antiochos, and C. R. DeVore, "Three-dimensional modeling of quasi-homologous solar jets," Astrophys. J. **714**, 1762 (2010).
[12]M. Yamada, in Proceedings of the 62nd Annual Meeting of the APS Division of Plasma Physics, Virtual Meeting, 2020.
[13]P. Bellan, *Spheromaks: A Practical Application of Magnetohydrodynamic Dynamos and Plasma Self Organization* (Imperial College Press, 2000).
[14]J. B. Taylor, Phys. Rev. Lett. **33**, 1139 (1974).
[15]T. Jarboe, I. Henins, A. R. Sherwood, C. W. Barnes, and H. W. Hoida, "Slow formation and sustainment of spheromaks by a coaxial magnetized plasma source," Phys. Rev. Lett. **51**, 39 (1983).
[16]S. C. Hsu and P. M. Bellan, "Experimental identification of the kink instability as a poloidal flux amplification mechanism for coaxial gun spheromak formation," Phys. Rev. Lett. **90**, 215002 (2003).
[17]C. R. Sovinec, J. M. Finn, and D. del Castillo-Negrete, "Formation and sustainment of electrostatically driven spheromaks in the resistive magnetohydrodynamic model," Phys. Plasmas **8**, 475 (2001).
[18]C. Munson, F. Janos, Wysocki, and M. Yamada, "Experimental control of the spheromak tilting instability," Phys. Fluids **28**, 1525–1527 (1985).
[19]J. M. Finn, W. M. Manheimer, and E. Ott, "Spheromak tilting instability in cylindrical geometry," Phys. Fluids **24**, 1336 (1981).
[20]A. Bondeson, G. Marklin, G. An, H. H. Chen, and Y. Lee, "Tilting instability of a cylindrical spheromak," Phys. Fluids **24**, 1682 (1981).
[21]J. M. Finn and A. Reiman, "Tilt and shift mode stability in spheromaks with line tying," Phys. Fluids **25**, 116 (1982).
[22]E. B. Hooper, C. A. Romero-Talamás, L. L. LoDestro, R. D. Wood, and H. S. McLean, "Aspect-ratio effects in the driven, flux-core spheromak," Phys. Plasmas **16**, 052506 (2009).

[23]E. V. Belova, S. C. Jardin, H. Ji, M. Yamada, and R. Kulsrud, "Numerical study of tilt stability of prolate field-reversed configurations," Phys. Plasmas **7**, 4996 (2000).
[24]T. Sato and T. Hayashi, "Externally driven magnetic reconnection and a powerful magnetic energy converter," Phys. Fluids **22**, 1189 (1979).
[25]J. Yee and P. M. Bellan, Phys. Plasmas **7**, 3625 (2000).
[26]C. E. Myers, E. V. Belova, M. R. Brown, T. Gray, C. D. Cothran, and M. J. Schaffer, "Three-dimensional magnetohydrodynamics simulations of counter-helicity spheromak mergin in the swarthmore spheromak experiment," Phys. Plasmas **18**, 112512 (2011).